First stages of silver electrodeposition in a Deep Eutectic Solvent. Comparative behavior in aqueous medium

P. Sebastián, E. Vallés, E. Gómez*,

Departament de Química Física and Institut de Nanociència i Nanotecnologia (IN^{2}UB), Universitat de Barcelona, Martí i Franquès 1, E-08028 Barcelona, Spain.

*Author to whom correspondence should be addressed

e-mail: e.gomez@ub.edu

Phone: 34 934 021 234

Fax: 34 934 021 231

Abstract

The aim of the present work was to study the viability of a deep eutectic solvent (DES) solvent (consisting in a eutectic mixture of 1 choline chloride: 2 urea) as electrolyte for the electrodeposition of silver (I), paying special attention to the influence of the liquid on the mechanism of nucleation process. As this DES solvent is rich in chloride anion, which can act as complexing agent of the silver cation, parallel analysis was made, as reference, in aqueous media, both in free-chloride solution and in excess of chloride. These studies were made to analyze the role of chloride anion on the first stages of silver electrodeposition, but also to compare as nucleation mechanism changes depending on the medium, especially when DES solvent was used. For all solutions, cyclic voltammetry was useful to establish the potential range at which silver electrodeposition occurred, while potentiostatic technique was used to study the mechanism of the process. In all media, the deposition follows a nucleation and three dimensional growth governed by diffusion. The viability of the nucleation mechanism by Scharifker-Hills model was demonstrated. The analysis of the rising parts of the j-t transients confirms the obtained results by the model. Diffusion coefficients of silver species present in the solution were calculated from linear regression of j vs $t^{-1/2}$ at long deposition times.

Keywords: silver electrodeposition, first stages, Deep Eutectic Solvent, chloride effect, nucleation

1. Introduction

In the last decades, room temperature ionic liquids (RTIL) have been demonstrated as an interesting alternative to the aqueous solutions for metals electrodeposition due to their intrinsic ionic conductivity, low vapor pressure and wide electrochemical window [1,2]. However, eutectic mixtures obtained by mixing quaternary ammonium halides with hydrogen bond donors, as amides, carboxylic acids or alcohols [3-6], known as deep eutectic solvents (DES) are emerging as substitutes of RTIL because of its lower price and greater stability against oxygen and water.

Metal deposition from DES liquids is an area that has received increasing interest. A wide range of metals has been electrodeposited from deep eutectic solvents [7-12]. However, these studies are generally limited to testing the possibility of electrodeposition and relatively little information is known about the general mechanism of nucleation, although efforts in this line appear in the literature [13-16].

As it is known, the electrodeposition of metals is remarkably dependent on the operating conditions, term that combines solution composition, substrate and current/potential applied. This is especially important when some of the components could act either as complexing agent of the electroactive species or as additive [17-19]. In the first situation, the reduction occurs at more negative potentials and in the second, the nucleation could be inhibited by adsorption on the electrode surface [17]. This could be the case of DES solvents when cations sensitive to species present in the bath are electrodeposited, the coexistence of different species with different capabilities could affect the nucleation process.

The purpose of this study is to study the mechanism of silver deposition in a DES and comparing it with the corresponding in aqueous media. The eutectic 1 choline chloride: 2 urea [3] is the selected DES. In aqueous medium, both perchlorate and chloride solutions were used; Ag(I) solubilises easily in perchlorate medium and in concentrated chloride solution, the excess of chloride allows the solubilisation of low Ag(I) concentration by means of Ag(I) complexation [20,21]. This last situation is comparable to that found in the ionic liquid in which a rough calculation indicates that the chloride concentration would be the equivalent of about 5 M, higher than the sodium chloride in aqueous medium [22]. The silver deposition in DES and in aqueous solution containing or not chloride complexing anion is analysed and compared.

2. Experimental

Chemicals used were silver nitrate from Panreac, sodium chloride and sodium perchlorate both from Merck, all of them of analytical grade. Aqueous solutions were prepared with water doubly distilled and then treated with a Millipore Milli-Q system and the pH was kept at 3. The DES solvent was prepared using choline chloride (from Across Organics) and urea (from Merck) of analytical grade. The solids, in the molar

proportion 1 choline chloride: 2 urea, were warmed and removed constantly to achieve the liquid state. In the solution prepared with DES no support electrolyte was added taking advantage that DES acts both as solvent and as support electrolyte. After preparation, these solutions were placed in a desiccator in order to avoid uptake of water by higroscopicity.

A cylindrical thermostatized three electrode cell of one single compartment was used. Electrochemical experiments were carried out using an Autolab with PGSTAT30 equipment and GPES software. Basic electrochemical study was made using vitreous carbon (from Metrohm) as working electrode, polished to a mirror finish using alumina of different grades (3.75 and 1.87 μm), cleaned ultrasonically for 2 min in water and dried with air prior to be immersed in the solution. The contact with the solution was by meniscus. The counter electrode was a spiral of platinum. The reference electrode was an Ag|AgCl/KCl 3M mounted in a Luggin capillary containing, upon depending the solvent, either $NaClO_4$ 0.6M, NaCl 3M in aqueous solutions or the DES solvent when it was worked in the ionic liquid medium. Stable and reproducible values of the potential were obtained with these reference electrodes [23].

Voltammetric experiments were carried out at 50 mV s^{-1}, scanning at first to negative potentials. Chronoamperometric experiments were performed starting from a potential where no process took place to the selected potential value. If the opposite is not said, all electrochemical experiments were made using freshly polished substrata. In aqueous media the working temperature was 25ºC, whereas the temperature selected in DES solvent was 70ºC to favour low viscosity and high conductivity of the solvent. Magnetic stirrer was used when the stirring effect was tested. Conductance of solution was measured using a Metrohm 660 conductometer.

Morphology was observed using a scanning electron microscope JEOL model JSM-6510.

3. Results and discussion

3.1 Aqueous media. Perchlorate salt

In order to establish the potential region in which the silver deposition takes place in the perchlorate medium the voltammetric curves for the process were recorded in a 1.0 10^{-3} M $AgNO_3$ + 0.6 M $NaClO_4$ solution. Voltammetric profile shows, in the negative scan, a sharp current increase that develops in a well-defined reduction peak which current decreases smoothly after exceeding the potential corresponding to the maximum. In the positive scan a single oxidation peak was recorded related to the silver oxidation (Fig 1 curve a). Reversing the scan at the initio of the negative current the typical loop associated to the nucleation and growth process was recorded (Fig. 1 curve b). Although all experiments were performed under a substrate freshly polished, reproducibility was getting hard and laborious given the low concentration of the electroactive species. For all experiments the Q_{ox}/Q_{red} ratio is greater than 85%, making in evidence the oxidizability of the deposit coherent to previous results [24].

The potentiostatic curves were recorded after applying a single step signal, from a potential at which no process occurs to potential values at which silver reduction takes place. All current transients exhibit the typical profile for nucleation and three dimensional growth, a current rising part that attains a maximum from which the current decays with increasing time. The comparison of the curves obtained at different potentials evidences that the current corresponding to the maximum (j_m) is greater as the overpotential increases, being the corresponding time at which the maximum appears (t_m) shortened (Fig 2A). For all potentials, the descending part of the transients overlapped, and plotting in logarithmic form, the current vs time curves adjust well to the known Cotrell equation [25] (Fig. 2A inset). Therefore, the process is controlled by the mass transfer of the electroactive species towards the electrode. Table 1 contains the corresponding calculated diffusion coefficients, values congruent with those previously reported in nitrate solution [26]. The mass control was experimentally demonstrated stirring the solution after a deposition time under stationary conditions: a sudden current increase was observed (Fig. 3) as consequence of the mass control effect on the process.

In order to establish the nucleation mechanism at the different potentials, the recorded j-t transients were compared with those provided by Scharifker and Hills theoretical model [27,28] This model proposes that, in dimensionless form, instantaneous nucleation (all nuclei immediately formed after the step potential) and progressive nucleation (nuclei formed according to kinetics) follow the equations:

$$\left(\frac{j}{j_{max}}\right)^2 = 1.9542\left(\frac{t}{t_m}\right)^{-1}\left[1-\exp\left(-1.2564\frac{t}{t_m}\right)\right]^2 \quad (1)$$

for instantaneous and:

$$\left(\frac{j}{j_{max}}\right)^2 = 1.2254\left(\frac{t}{t_m}\right)^{-1}\left[1-\exp\left(-2.3367\left(\frac{t}{t_m}\right)^2\right)\right]^2 \quad (2)$$

for progressive.

The comparison of the non-dimensional plots with the corresponding to limit situations of progressive and instantaneous nucleation shows that the silver nuclei were formed instantaneously after applying sufficient overpotential and the curve perfectly superposes on that of arrested nucleation process, whereas at the lower overpotentials, intermediate nucleation behavior is observed (Fig. 2B).

Other authors detect also instantaneous silver nucleation at high overpotentials [18,19,29,30]. Taking into account that, in the actual experimental conditions, the silver (I) concentration was lower than the used on the referred works, the detection of intermediate nucleation at the lower overpotentials could be justified.

3.2 Aqueous media. Chloride as complexing agent

Due to the lower solubility of the ion Ag (I) in chloride, the stable solution prepared was $AgNO_3$ 1.0 10^{-3} M + NaCl 3.0 M because lower NaCl concentration leads to solution instability after a few days. The voltammograms from this concentrated chloride medium shows that the process begins at considerable more negative potential (Fig 1 curve c) than in perchlorate solution. This delay could be assigned to the formation of the main $[AgCl_4]^{3-}$ complex [21]. Although the voltammetric profiles were quite similar than the recorded in perchlorate medium, the total charge involved was smaller. Reversing the scan, the characteristic nucleation and growth loop was also observed (Fig 1 curve d).

Figure 4A shows the j-t transients recorded at different overpotentials; the transients show the mass control process. As the potential becomes more negative, the silver nucleation and growth current increases leading an increase of j_m and a decrease of t_m. As occurred in the free-complex solution the final part of the transients converge, being

the calculated diffusion coefficient (Table 1), for the silver-complexed species, a little lower than the obtained for the uncomplexed one calculated from the perchlorate solution. This agrees with the lower charge recorded under the voltammetric curve from the chloride solution respect to that recorded in perchlorate solution.

As occurs in the free-complex solution, progressive nucleation was observed at the lowest overpotentials. Upon increasing slightly the overpotential, instantaneous nucleation was observed (Fig 4B). The change from progressive to instantaneous takes place abruptly in a narrow potential range. This abrupt change of behavior could be interpreted accepting that as the potential was made more negative, the repulsion between the complex negatively charged and the electrode favors the lost of the chloride crown and the bare ion find a substrate with a very favorable potential conditions allowing all the nucleation sites coverage instantaneously.

For this solution, the results obtained for the nucleation mechanism from the SH model were also compared with those extracted from the logarithmic adjustment of the rising part of the j-t transients, according to the equation

$$j = \frac{2}{3} zF\pi (2Dc)^{3/2} M^{1/2} \rho^{-1/2} N_o A t^{3/2} \qquad (3)$$

derived assuming progressive nucleation, and as:

$$j = zF\pi (2Dc)^{3/2} M^{1/2} \rho^{-1/2} N_o t^{1/2} \qquad (4)$$

for instantaneous one

where zF is the molar charge of the depositing species, D is the diffusion coefficient, c is the concentration in mol cm^{-3}, M is the molecular weight and ρ is density, N_o is the maximum number of nuclei obtainable under the prevailing conditions and A is the steady state nucleation rate constant per site [27].

The adjustment was made for all the transients recorded, except for those obtained at the highest overpotentials, for which no enough data were available. Even at the lowest overpotentials, the calculated slopes from the logarithmic plot were smaller of 3/2, whereas increasing the overpotential the slope was approaching to 1/2 (Fig. 5). This supports the results previously obtained from the SH model.

The chloride presence delays the silver nucleation and growth deposition process and when the deposition potential is sufficiently negative to favor the bareness of the ion instantaneous nucleation is achieved. Chloride presence, at sufficient negative potential did not affect the substrate surface.

3.3 Deep eutectic solvent

The objective of this section is to analyze the first stages of silver deposition process in the DES solvent. The high viscosity and low conductivity of the DES discouraged the experiments at room temperatures (25ºC) especially when low concentrations of electroactive species are required [2,31]. The effect of temperature over the solvent conductivity was determined in order to select an adequate temperature for deposition. Conductivity increases rising the temperature (Fig. 6). The selection of 70ºC as operative temperature was considered as a good choice because the conductivity rises ten times respect to that at 25ºC. Simultaneously, a decrease of the viscosity was observed as has been previously evaluated [3].

Although our first attempt was to compare the mechanism of silver deposition in different media at fixed Ag(I) concentration, very low current was detected in DES (at noise level) for Ag(I) concentration in the millimolar range. Then, solutions between twenty (0.02 M) and fifty times (0.05 M) higher have been prepared for Ag deposition in DES. These Ag(I) concentrations were far superior and not available in aqueous medium using chloride as complexing agent.

Silver deposition voltammetric profiles in DES solvent were similar than in aqueous media: reduction peak, single oxidation peak (Fig. 7A) and the typical nucleation loop (inset Fig. 7A). However, a careful comparison with the profiles obtained in aqueous medium reveals: a) that the voltammetric reduction peak appears at potentials noticeably more negative than those in aqueous medium and b) that the increase of current previous to the maximum of the reduction peak proceeds slower than in aqueous medium. The sharp current decay observed in aqueous media does not appear here; the reduction peak is smoother than those recorded in aqueous media. Similar behavior was observed for both concentrations studied.

In order to investigate if the differences in the reduction peak profile were related to substrate surface, different treatments were applied to attain possible improvement of

surface preparation. In the most exhaustive treatment, substrate was prior oxidized at +0.8 V during 150 s, in order to ensure that the residual oxidation current was very low, and then it was mechanically polished with alumina according to the protocol described in experimental section. Different substrate preparation leads to superimposable voltammetries; reproducible curves were obtained, both in shape and involved charge (Fig. 7B), which confirms the reliability of the recorded curves.

Lengthening the negative scan to more negative values a new band appears previous to massive reduction of DES solvent (Fig.8A). To establish the origin of this band, which doesn't appear in the blank solution (DES solvent only) using vitreous carbon (Fig.8B curve a), a voltammetric study was performed in the blank solution using as working electrode silver freshly deposited over vitreous carbon. In the negative scan, a current band centered at 1.47 V was detected; previous to the massive current related to the reduction of DES solvent over the silver freshly deposited (Fig. 8B curve b). It was confirmed that this band was associated to the presence of metallic silver: silver advances the appearance of current corresponding to solvent reduction. Similar advancement of the current onset was previously detected over other metallic substrata [32], being the current band assigned to hydrogen formation from the hydrogen donor species that constituted the solvent [33]. Therefore, the detected band was not related to silver reduction processes. The silver presence modifies the reduction solvent process.

Established the potential range at which silver deposition process occurs, chonoamperometric curves were recorded (Fig. 9A and 9B). The shape of the j-t transients shows tridimensional growth. The profiles are similar to the corresponding to nucleation and growth process controlled by mass transfer obtained previously in aqueous solution. The reproducibility of the experiments was satisfactory and the transients merged also to the same current value at long deposition times. However, the j_m and t_m changes associated to the overpotential modification are slower than those observed in aqueous media. The interval of applied potential necessary to allow similar change percentage in the recorded current widens respect to the needed in aqueous solution, as the manner that very high overpotentials have had to apply to attain fast processes.

The excellent concordance of the descending parts of the all j-t transients recorded in the DES for the silver deposition allows determining, as in aqueous media, the diffusion

coefficient of Ag(I) species through Cottrell equation. For all Ag(I) concentrations in DES, linear relation between logarithmic values of both current and deposition time were obtained, with a slope close to -0.5. The plots for fixed concentration and different potentials were quasi coincident (Fig.10). The obtained diffusion coefficients were two magnitude orders lower than those calculated in aqueous medium (Table 1) and in concordance with those obtained using other ionic liquids [34]. Results expected, given the stationary currents values recorded, that were comparable to those obtained in aqueous media although the concentration and temperature were higher.

The comparison of the non-dimensional plots according to SH model confirms the availability of the model for the analysis of the process in this medium. For [Ag(I)]= 0.05 M, silver deposition adjusts to near progressive nucleation at the lowest applied overpotentials, whereas increasing the overpotential the nucleation mechanism move away to intermediate behavior (Fig. 9C). Overpotential of -450 mV was no sufficient to attain instantaneous nucleation. Higher overpotentials were not considered in order to avoid the possible interference of DES reaction on the freshly silver deposited.

Fitting the plots recorded from the [Ag(I)]= 0.02 M solution (Fig. 9D), instantaneous behavior was not achieved, even at the highest overpotentials, although the curves are closer than for [Ag(I)]= 0.05 M. Moreover, surprisingly, an accurate inspection of the descending part of the non dimensional transients at greater deposition times shows that the curves smoothly approach to progressive nucleation behavior, more evident as the overpotential increases.

As complementary study of the previous non dimensional analysis by SH model, the rising part of the j-t transients was analyzed for [Ag(I)]= 0.05 M according to the equations (3) and (4). A linear dependence was observed for all plots (Fig. 11), being the calculated slope values between 1.2 at the lowest overpotential and 0.58 for the highest one. This suggests an intermediate nucleation behavior, as was obtained according to SH model.

The type of nucleation process can also be derived from the j_m and t_m values of the j-t transients (Table 2). The theory requires that $j_m^2 * t_m$ be equal to of 12.58 10^{-7} A^2 cm^{-4} s for progressive and of 7.89 10^{-7} A^2 cm^{-4} for arrested nucleation [27,35]. The calculated $j_m^2 * t_m$ products (Table 2) confirm intermediate behavior, with slow transition to progressive from instantaneous nucleation. The values obtained at the lowest

overpotential close well with those predicted for progressive nucleation and the obtained at the high overpotential tested (E= -850 mV) approaches significantly to those predicted for instantaneous. Better fitting was attained at low overpotentials, for which t_m is greater and the measured current is affected by the double layer discharge current only for the very initial times.

From the different analysis performed, we can conclude that silver deposition process in the selected DES corresponds to a nucleation and tridimensional growth controlled by diffusion, which nucleation evolves from progressive to instantaneous upon increasing the overpotential. The slow evolution to instantaneous nucleation seems to indicate that the liquid presence causes, in addition to the complexation of the silver (I), a modification in the surface substrate that hinders the formation of the first nucleus.

3.4 Morphological study

In order to analyze the role of the composition of the DES solvent over the growth of silver electrodeposits, and leading especial attention to the chloride presence effect, a morphological analysis was performed. As reference, deposits in aqueous medium (perchlorate and chloride) were prepared in parallel conditions.

Figure 12A shows that silver deposition from the DES solvent begins by isolated grains, some of them forming twinned chains along the substrate. Increasing the deposition charge (Fig. 12B) the deposit was formed by small blocks covering all the substrate. Deposits obtained slowly at long deposition time are formed by platelets on which growth in the z-axis seems hindered (Fig. 12C). It seems that DES medium hinders the vertical growth of the silver deposit.

When silver deposits were grown in aqueous medium (chloride (Fig. 12D) and perchlorate (Fig. 12E)) clear effect of the chloride presence can be observed: excess of chloride anion in solution favored the formation of smaller and flatter crystals respect to perchlorate medium, probably due to the adsorption of chloride during silver growth. Chloride anion hinders the 3D growth of silver crystals [30,36]. On the other hand, both in perchlorate and in chloride medium, absence of little grains was observed on the substrate as corresponds to a high superficial mobility of the nucleus formed.

Silver growth in DES and aqueous chloride medium was vertically hinder. However, more rounded grains of smaller size were obtained in DES respect to aqueous chloride

medium. This fact can be interpreted for the lower superficial diffusion in DES, more viscous solvent [37]. The different shape observed in both cases could be related to the different superficial tension silver deposit/solution.

3.5 Substrate activation

In previous section was demonstrated that silver electrodeposition on vitreous carbon in the DES solvent can be explained on the basis of intermediate nucleation mechanism. As this mechanism can be affected by superficial state of the substrate, a parallel study was made with a substrate preparation that did not involve mechanical polishing, in order to check how the state of the surface could affect the nucleation mechanism.

When consecutive voltammetric scans were performed, silver reduction process advances, especially between the first and the second scan (Fig. 13). Moreover, from the second scan the shape of the reduction peak changes, it develops fast, as corresponds to greater nucleation and growth rate.

To analyze the nucleation mechanism, potentiostatic experiments were made on the vitreous carbon electrode prepared only by applying a potential of 0.8 V until the recorded oxidation current was negligible.

The j-t transients show the typical profile of nucleation and three dimensional growth (Fig. 14A) for processes controlled by mass transfer with the usual effect of the overpotential. The analysis by SH model indicates that even at intermediate overpotentials instantaneous nucleation was detected, unlike the results obtained using the same substrate mechanically polished with alumina.

Although during the new method of substrate preparation, the potential was applied until no relevant oxidation current was recorded (lower than 10^{-7} A), the substrate should be marked in some way, such that the consequent nucleation was favoured. Therefore, nucleation sites are activated, so that the sites previously occupied act as seed for the nucleation in subsequent experiment. This effect well known in aqueous media, in the DES solvent acquire an interesting application when the deposit formation would require instantaneous nucleation.

4. Conclusions

This work reports the electrodeposition of silver from a eutectic mixture of choline chloride-urea. The electrochemical reduction was studied by cyclic voltammetry and the nucleation and growth process was investigated by potentiostatic technique. Similar analysis was made in aqueous solution with and without chloride ion in excess.

Both chronoamperometric and voltammetric results make in evidence that the silver deposition in all conditions studied corresponds to a 3D nucleation and growth process, diffusion controlled.

The use of DES as solvent slows the growth process, the recorded current are lower than the obtained in aqueous medium. In the DES solvent comparable current values were obtained using higher both temperature and concentrations and sufficient overpotential.

It was demonstrated the applicability of the SH model in the DES solvent, that makes in evidence that the silver deposition process is affected by the presence of the solvent species especially in the DES media. Whereas in aqueous medium instantaneous behaviour is attained even at moderate overpotentials, extreme overpotential conditions are needed to close approaching to instantaneous nucleation in the DES solvent. It is necessary using "marked"/activated electrode to attain instantaneous nucleation at moderate overpotentials.

The morphological study demonstrates the inhibitory effect of chloride on the deposit's growth, both in aqueous solution and DES solvent. Chloride presence hinders the uncontrolled directional growth observed in the free-chloride solution. However, in the DES solvent, the morphology of the obtained deposits also shows the effect of the different both superficial diffusion and surface tension of the silver/solution interface, which leads deposits with rounded grains at low deposition times and smoother edges in the crystallites at longer ones.

It can be concluded from the present work that the components of the eutectic mixture affect both the first stages and the growth of the deposit. The quantitative analysis shows that the process hardly reaches instantaneous nucleation, unlike what occurs in aqueous media. The morphological analysis evidences that the characteristic nature of

DES affects the growth process in addition to the inhibitory effect of the chloride observed in aqueous medium.

Acknowledgements

This paper was supported by contract CTQ2010-20726 (subprogram BQU) from the *MINECO*. The authors wish to thank the *Centres Científics i Tecnològics de la Universitat de Barcelona (CCiTUB)* for the use of their equipment.

References

[1] Electrochemical Aspects of Ionic Liquids, in. Hiroyuki Ohno (Ed), John Wiley & Sons, Hoboken, New Jersey, 2005.

[2] A. Hentz, C. Wertz. Pure Appl. Chem. 78 (2006) 778.

[3] A.P. Abbott, G. Capper, D.L. Davies, R.K. Rasheed, V. Tambyrajah, Chem. Comm. (2003) 70.

[4] A.P. Abbott, D. Boothby,G. Capper, D.L. Davies, R.K. Rasheed, J. Am. Chem. Soc. 126 (2004) 9142.

[5] A.P. Abbott, G. Capper, K.J. McKenzie, K. S. Ryder, J. Electroanal. Chem. 599 (2007) 288.

[6] A. Florea, L. Anicai, S. Constonci, F. Golgovici, T. Visan, Surf. Interface Anal. 42 (2010) 1271.

[7] A.P. Abbott, G. Capper, K.J. McKenzie, A. Glidie, K. S. Ryder, Phys. Chem. Chem. Phys. 8 (2006) 4214.

[8] A.P. Abbott, J. Griffith, S. Nandhra, CO'Connor, S. Postlethwaite, K.S. Ryder, E.L. Smith, Surf Coat Technol. 202 (2008) 2033.

[9] K. Haerens, E, Matthijs, A. Chmielarz, Bart van der Bruggen, J. Environmental. Management 90 (2009) 3245.

[10] P.J. Dale, A.P. Samantilleke, D.D. Shivagan, L.M. Peter, Thin Solid Films 515 (2007) 5751.

[11] M. Steichen, M. Thomassey, S. Siebentritt, P.J. Dale, Phys. Chem. Chem.Phys, 13 (2011) 4292.

[12] P. Guillamat, M. Cortes, E. Valles, E. Gomez, Surf. Coat. Technol. 206 (2012) 4439.

[13] N. M. Pereira, P. M. V. Fernades, C. M. Perreira, A. F. Silva. J. Electrochem. Soc. 159 (2012) D-501.

[14] H.Y. Yang, X.W. Guo, X.B. Chen, S.H. Wang, G.H. Wu, W.J. Ding, N. Birbilis, Electrochim. Acta 63 (2012) 131.

[15] A.P. Abbott, K.El Ttaib, G. Frisch, K.J. McKenzie, K. S. Ryder, Phys. Chem. Chem. Phys. 11 (2009) 4269.

[16] T. Tsuda, L.E. Boyd, S. Kuwabata, Ch. L. Hussey, J. Electrochem. Soc., 157 (8) (2010) F96.

[17] G.M. Zarkadas, A. Stergiou, G. Papanastasiou. J. Appl. Electrochem. 31 (2001) 1251.

[18] K. Márquez, G. Staikov, J. W. Schultze. Electrochim. Acta. 48 (2003) 875.

[19] Z. B. Lin, B. G. Xie, J. S. Chen, J. J. Sun, G. N. Chen. J. Electroanal. Chem. 633 (2009) 207.

[20] Crytical Stability Constants in: A. E. Martell, R. M. Smith vol. 5 pag. 419, Plenum Press, New York, 1982.

[21] MEDUSA-Chemical Diagrams (2.0) and HYDRA-Hydrochemical Database (2.0). Softwares of I. Puigdomenech. http://www.kemi.kth.se/medusa/.

[22] Crytical Stability Constants in: A. E. Martell, R. M. Smith vol. 6 pag. 455, Plenum Press, New York, 1982.

[23] E. Gomez, P. Cojocaru, L. Magagnin, E. Valles, J. Electroanal. Chem. 658 (1-2) (2011) 18.

[24] A. Basile, A. I. Bhatt, A. P. O'Mullane, S. K. Bhargava. Electrochim. Acta. 56 (2011) 2895.

[25] A. A. F. Bard, R. Larry. Electrochemical methods: fundamentals and applications. Second edition. John Wiley & Sons Inc. New York. (1980) 163.

[26] J. Mostany, B.R. Scharifker, K. Saavedra, C. Borras, Russian J. Electrochem. 44 (2008) 652.

[27] G. Gunawardena, G. Hills, I. Montenegro, B. Sharifker, J. Electroanal. Chem. 138 (1982) 225.

[28] B. Scharifker, G. Hills, Electrochim. Acta. 28 (1983) 879.

[29] A. Milchev, B. Sharifker, G. Hills. J. Electroanal. Chem. 132 (1982) 277.

[30] C. Ramirez, E. M. Arce, M. Romero-Romo, M. Palomar-Pardavé. Solid State Ionics. 169 (2004) 81.

[31] S. I: Fletcher, F. B. Sillars, N. E. Hudson, P. J. Hall. J. Chem. Eng. 55 (2010) 778.

[32] E. Gomez, E. Valles Int. J. Electrochem. Sci., 8 (2013) 1443.

[33] D. Yue, Y. Jing, Y. Yao, J. Sun, Y. Jia, Electrochim. Acta. 65 (2012) 30.

[34] A.W. Taylor, P. Licence, A. P. Abbott. Phys. Chem. Chem. Phys. 13 (2011) 10147.

[35] G. Gamini, G. Gunawardena, G. Hills. J. Electroanal. Chem. 138 (1982) 241.

[36] X. H. Xu, C. L. Hussey. J. Electrochem. Soc. 139 (1992) 1298.

[37] A. P. Abbott, K. E. Tttaib, G. Frisch, K. S. Ryder, D. Weston. Phys. Chem. Chem. Phys. 14 (2012) 2443.

Captions for Figures

Fig. 1. Voltammetric curves at 50 mVs^{-1} at different negative limits from: 1 10^{-3} M $AgNO_3$ + 0.6 M $NaClO_4$ solution a) -100 mV and b) 215 mV (nucleation loop), and from 1 10^{-3} M $AgNO_3$ + 3.0 M NaCl solution curves: c) -500 mV and d) -185 mV (nucleation loop).

Fig. 2. A) Potentiostatic current transients for the deposition of silver from 1 10^{-3} M $AgNO_3$ + 0.6 M $NaClO_4$ solution, curves a) 225, b) 210, c) 165, d) 155, e) 135, f) 120 and g) 105 mV. Inset 2A Plots according Cotrell equation for curves d, f and g. B) Non-dimensional plots of $(I/I_m)^2$ vs t/t_m for some of j-t transients of figure 2A.

Fig. 3. Potentiostatic current transient for the deposition of silver from 1 10^{-3} M $AgNO_3$ + 0.6 M $NaClO_4$ solution at 170 mV under a) stationary and b) stirred conditions.

Fig. 4. A) Potentiostatic current transients for the deposition of silver from 1 10^{-3} M $AgNO_3$ + 3.0 M NaCl solution, curves a) -155, b) -160, c) -175, d)-180 and e) -200 mV. B) Non-dimensional plots for all transients of figure 4A.

Fig. 5. Current vs time, logarithmic plot of rising part of the current transients for the deposition of silver from 1 10^{-3} M $AgNO_3$ + 3.0 M NaCl solution, curves a) -155, b) -165 and c) -175 mV.

Fig. 6. Specific conductivity-temperature dependence for DES solvent

Fig. 7.A) Voltammetric curves at 50 mVs^{-1} at different Ag(I) concentrations, curves: a) 2 10^{-2} and b) 5 10^{-2} M $AgNO_3$ in the DES solution. Inset: nucleation loop for 5 10^{-2} M $AgNO_3$ solution. B) Voltammetric curves recorded: solid line habitual polishing treatment, dashed line oxidation plus polishing treatment.

Fig. 8. A)Voltammetric curve at 50 mVs^{-1} from 5 10^{-2} M $AgNO_3$ in the DES solution. B) voltammogram details from the blank solution curves: a) vitreous carbon and b) on Ag freshly deposited.

Fig. 9. Potentiostatic current transients for the deposition of silver in DES solvent from: A) 5 10^{-2} M $AgNO_3$ curves a) -400, b) -450, c) -500, d) -550, e) -600, f) -650, g) -700, h) -750, i) -800 and j) 850 mV. B) 2 10^{-2} M $AgNO_3$ curves a) -550, b) -650, c) -750, d) -850 and e) 900 mV. C) and D) Non-dimensional plots for the transients of figure 9A and 9B respectively.

Fig. 10. Cotrell plots for some transients of figures a) 9A and b) 9B.

Figure 11. Logarithmic plots of the rising part of the j-t transients obtained at 5 10^{-2} M $AgNO_3$ in the DES solvent. a) -400, b) -450, c) -500, d) -550, e) -600, f) -650, g) -750, h) -800 and i) 850 mV.

Figure 12. SEM images of silver deposits prepared potentiostatically from solutions prepared: in the DES solvent A) at -400 mV, Q=10 mC, B) at -400 mV, Q=35 mC , C) at -500 mV, Q=50 mC w=0, in aqueous media D) chloride at -170 mV, Q=15 mC and E) perchlorate at -220 mV, Q=65 mC.

Figure 13. Consecutive voltammetric curves at 50 mVs^{-1} from 5 10^{-2} M $AgNO_3$ in the DES solution.

Fig.14. A) Potentiostatic current transients for the deposition of silver in DES solvent from: 5 10^{-2} M $AgNO_3$ curves a) -450, b) -550, c) -650. B) Non-dimensional plots for the transients of figure 14A.

Table 1. Averaged diffusion coefficients obtained from the descending part of the j-t transients in the analyzed solutions.

ClO_4^- medium	Cl^- medium	DES Solvent	
[Ag(I)]=0.001 M	[Ag(I)]=0.001 M	[Ag(I)]=0.02 M,	[Ag(I)]=0.05 M
2.51E-05 cm^2 s^{-1}	1.33E-05 cm^2 s^{-1}	2.06E-07 cm^2 s^{-1}	2.40E-07 cm^2 s^{-1}

Table 2. Characteristics of the potentiostatic current maximum for the potentiostatic transients obtained from [Ag(I)]=0.05M solution in the DES solvent.

E/mV	j_m/Acm^{-2}	t_m/s	j_m^2*t_m
-850	-1.68E-03	0.303	8.58E-07
-800	-1.28E-03	0.548	8.92E-07
-750	-1.14E-03	0.774	9.99E-07
-700	-1.01E-03	0.950	9.64E-07
-600	-7.62E-04	1.650	9.58E-07
-550	-6.51E-04	2.459	1.04E-06
-500	-5.58E-04	3.250	1.01E-06
-450	-4.69E-04	5.000	1.10E-06
-400	-3.70E-04	8.950	1.23E-06

Table 1. Averaged diffusion coefficients obtained from the descending part of the j-t transients in the analyzed solutions.

ClO_4^- medium	Cl^- medium	Deep Eutectic Solvent	
[Ag(I)]=0.001 M	[Ag(I)]=0.001 M	[Ag(I)]=0.02 M,	[Ag(I)]=0.05 M
2.51E-05 cm^2 s^{-1}	1.33E-05 cm^2 s^{-1}	2.06E-07 cm^2 s^{-1}	2.40E-07 cm^2 s^{-1}

Table 2. Characteristics of the potentiostatic current maximum for the potentiostatic transients obtained from [Ag(I)]=0.05M solution in the DES solvent.

E/mV	j_m/A cm^{-2}	t_m/s	j_m^2*t_m
-850	-1.68E-03	0.303	8.58E-07
-800	-1.28E-03	0.548	8.92E-07
-750	-1.14E-03	0.774	9.99E-07
-700	-1.01E-03	0.950	9.64E-07
-600	-7.62E-04	1.650	9.58E-07
-550	-6.51E-04	2.459	1.04E-06
-500	-5.58E-04	3.250	1.01E-06
-450	-4.69E-04	5.000	1.10E-06
-400	-3.70E-04	8.950	1.23E-06

* E is referred to Ag/AgCl/Cl$^-$ electrode

Figure 1
Click here to download high resolution image

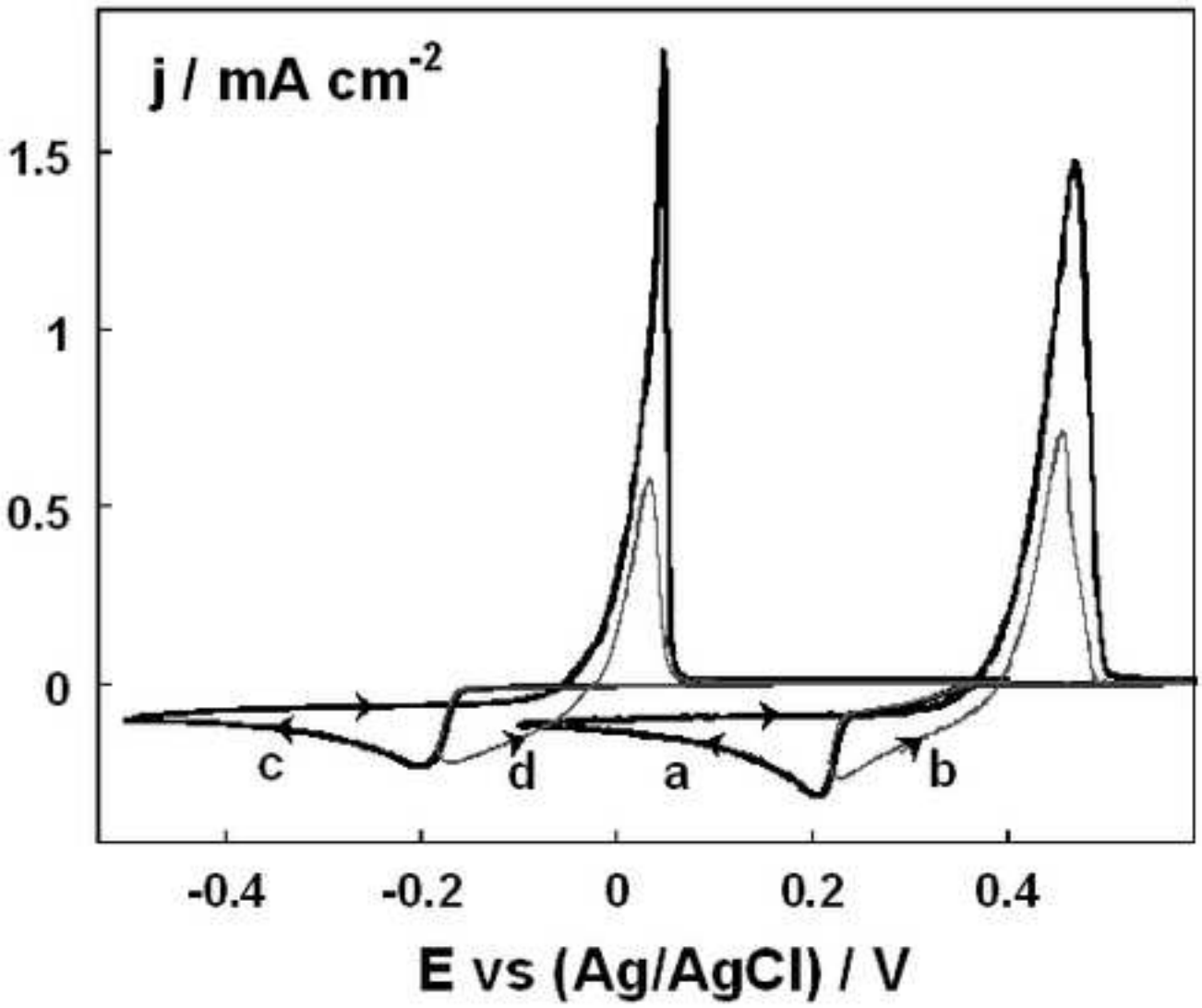

Figure 1

Figure 2
Click here to download high resolution image

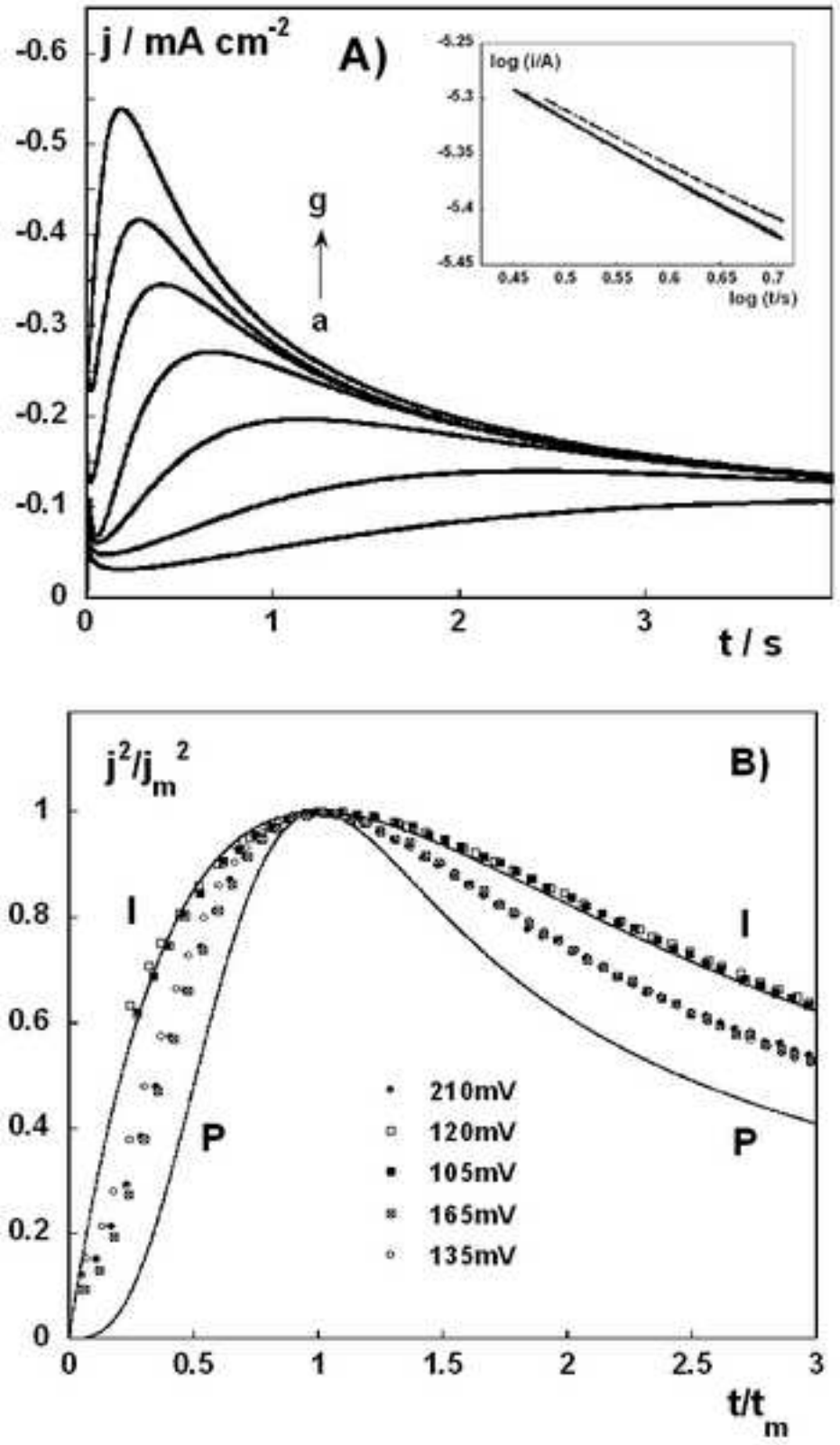

Figure 2

Figure 3
Click here to download high resolution image

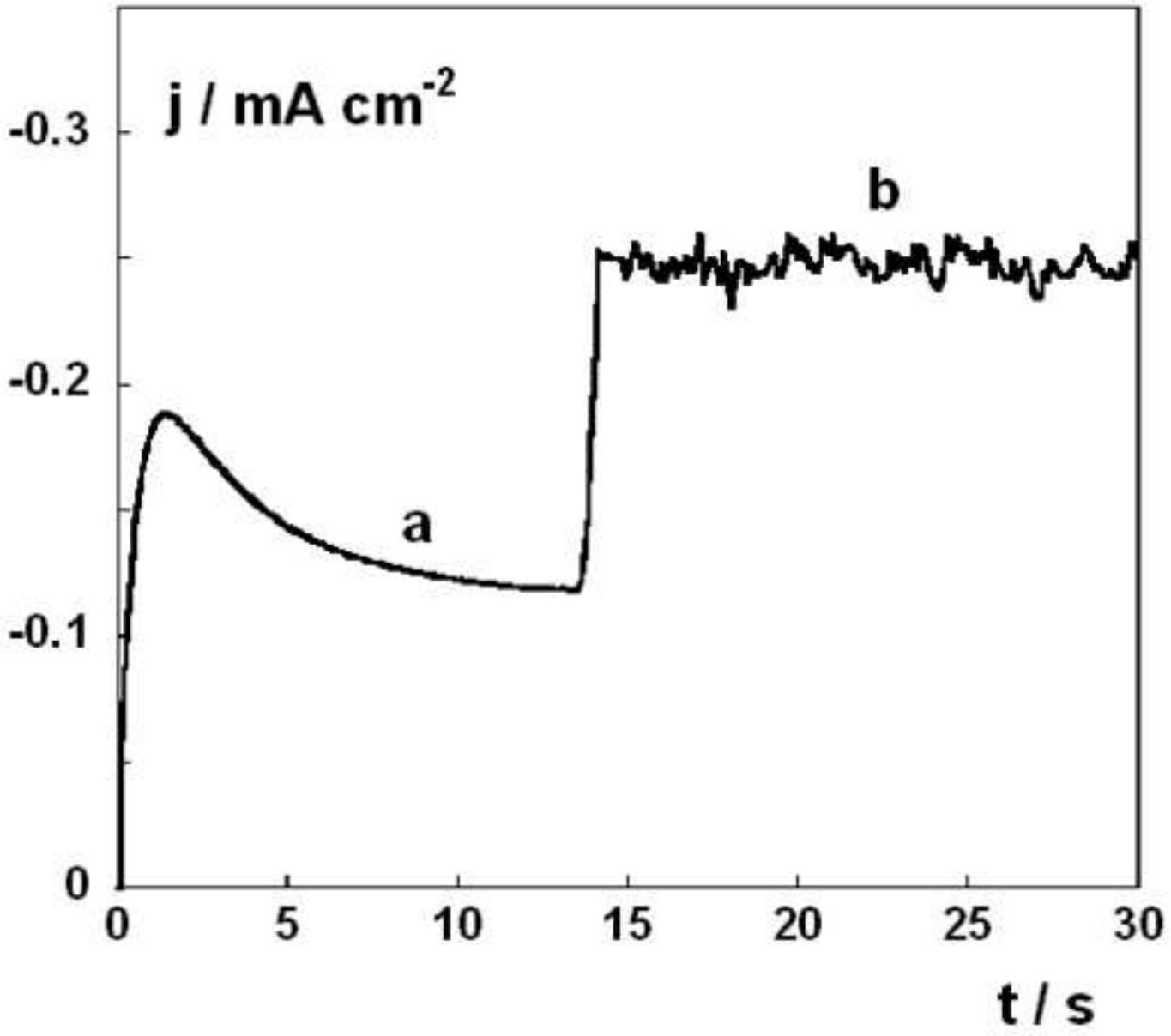

Figure 3

Figure 4
Click here to download high resolution image

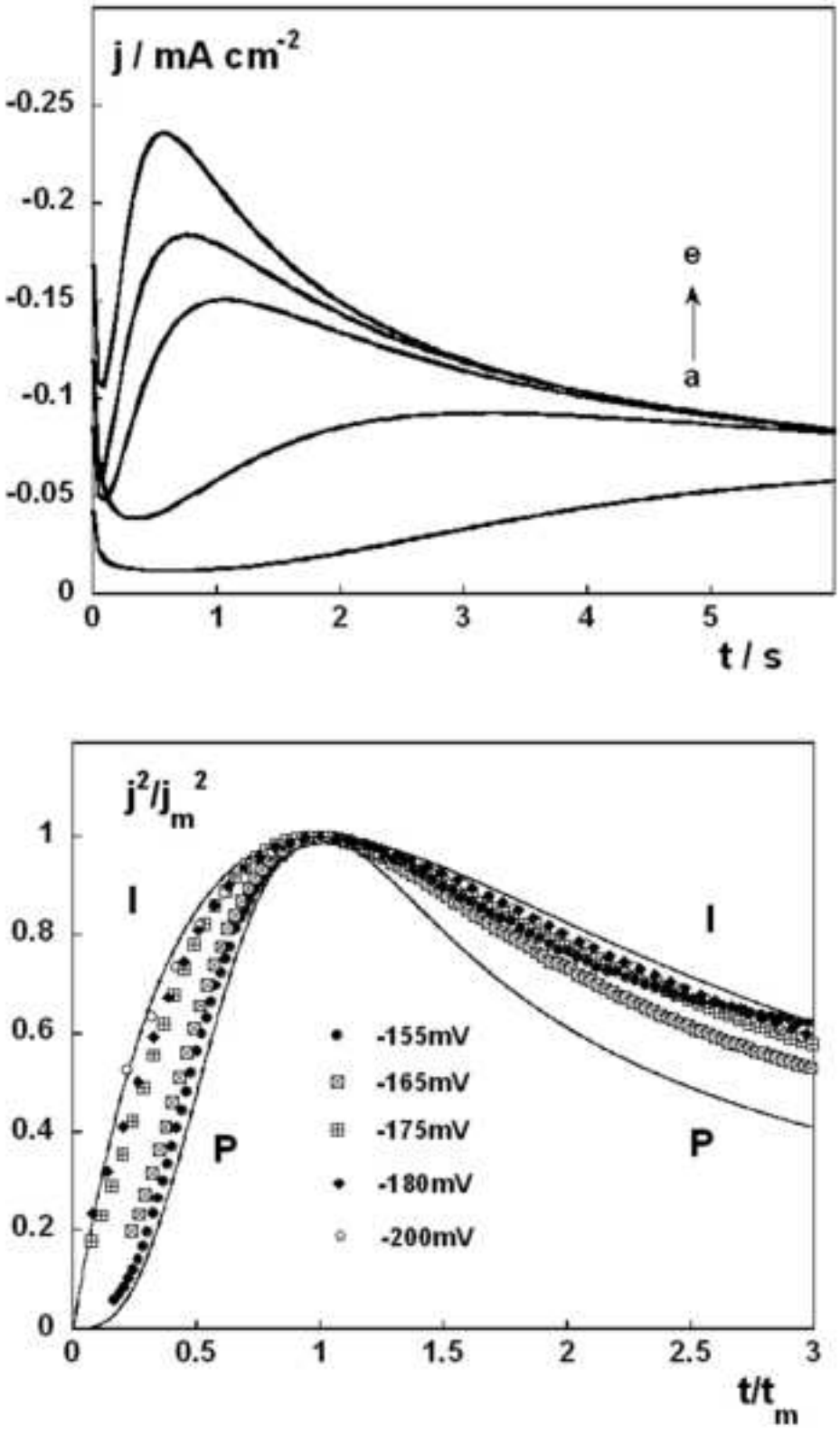

Figure 4

Figure 5
Click here to download high resolution image

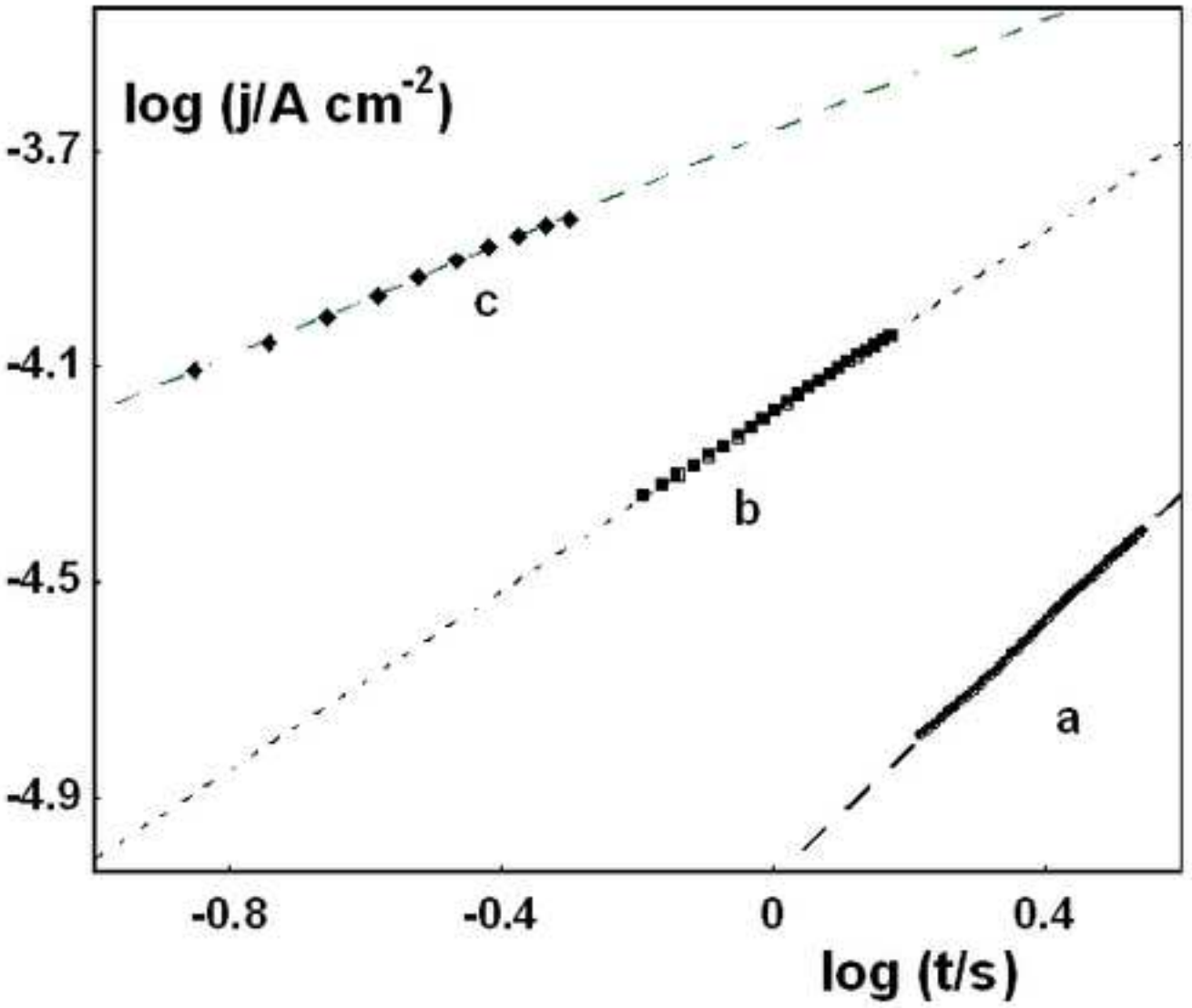

Figure 5

Figure 6
Click here to download high resolution image

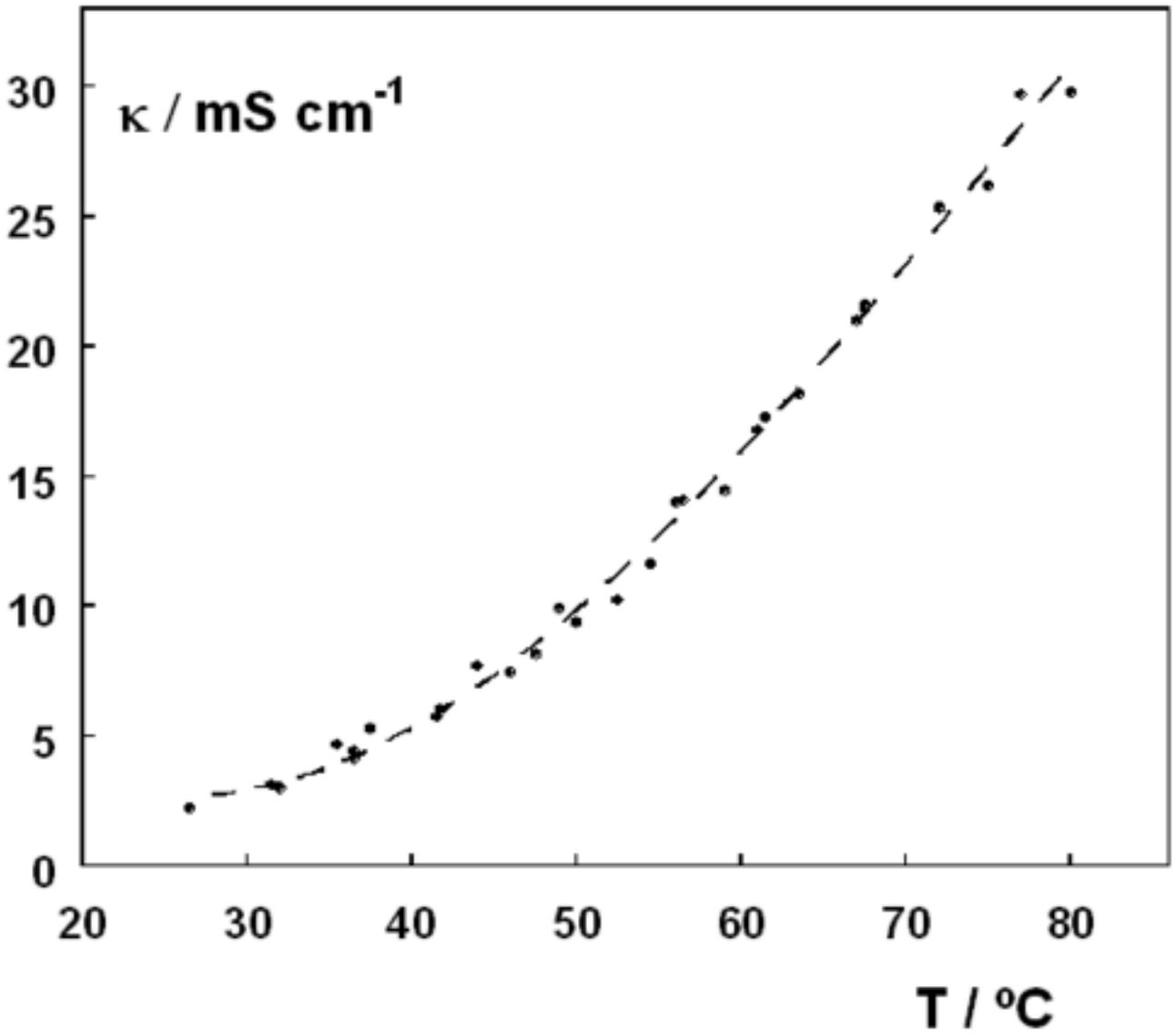

Figure 6

Figure 7
Click here to download high resolution image

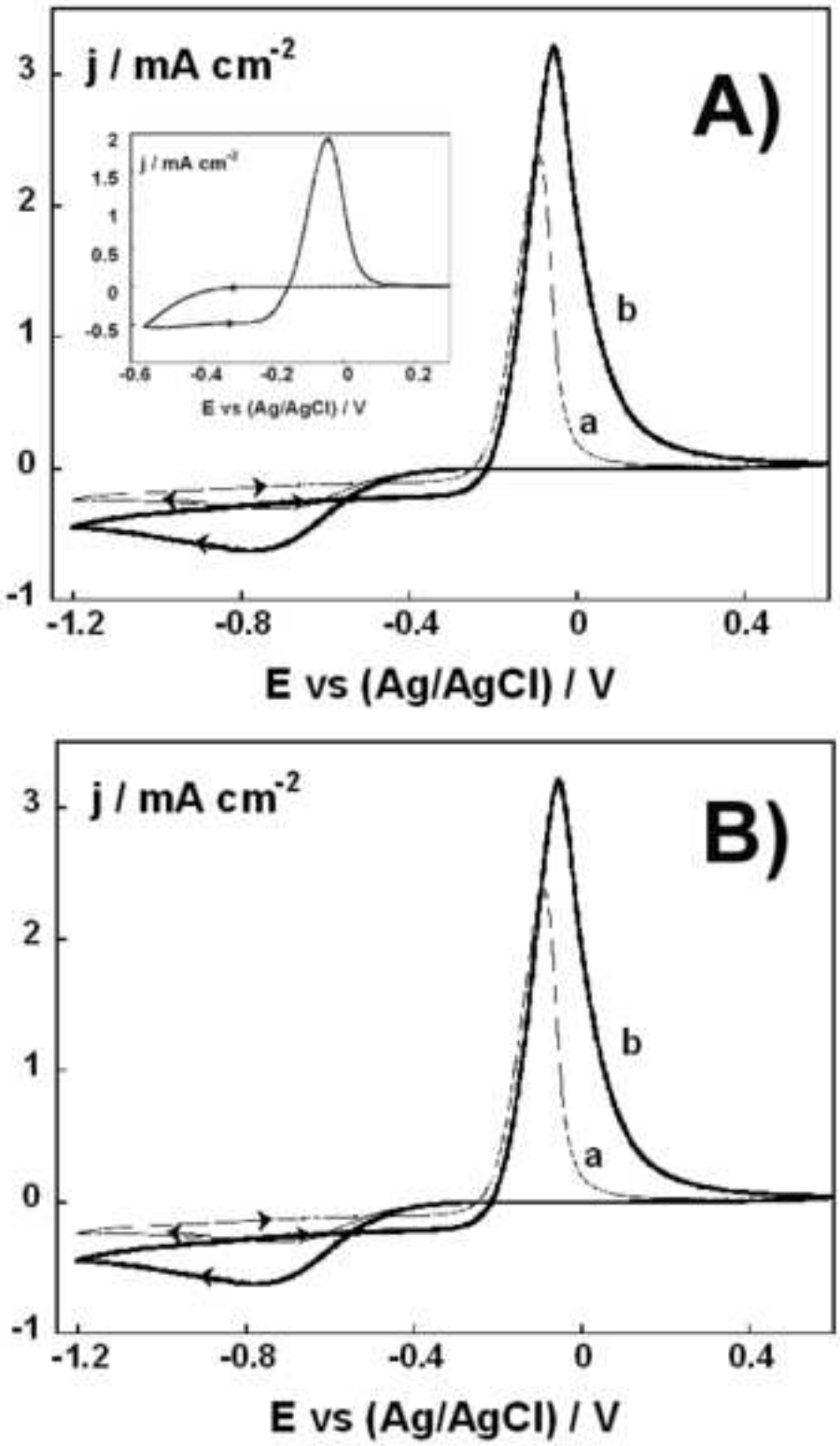

Figure 7

Figure 8
Click here to download high resolution image

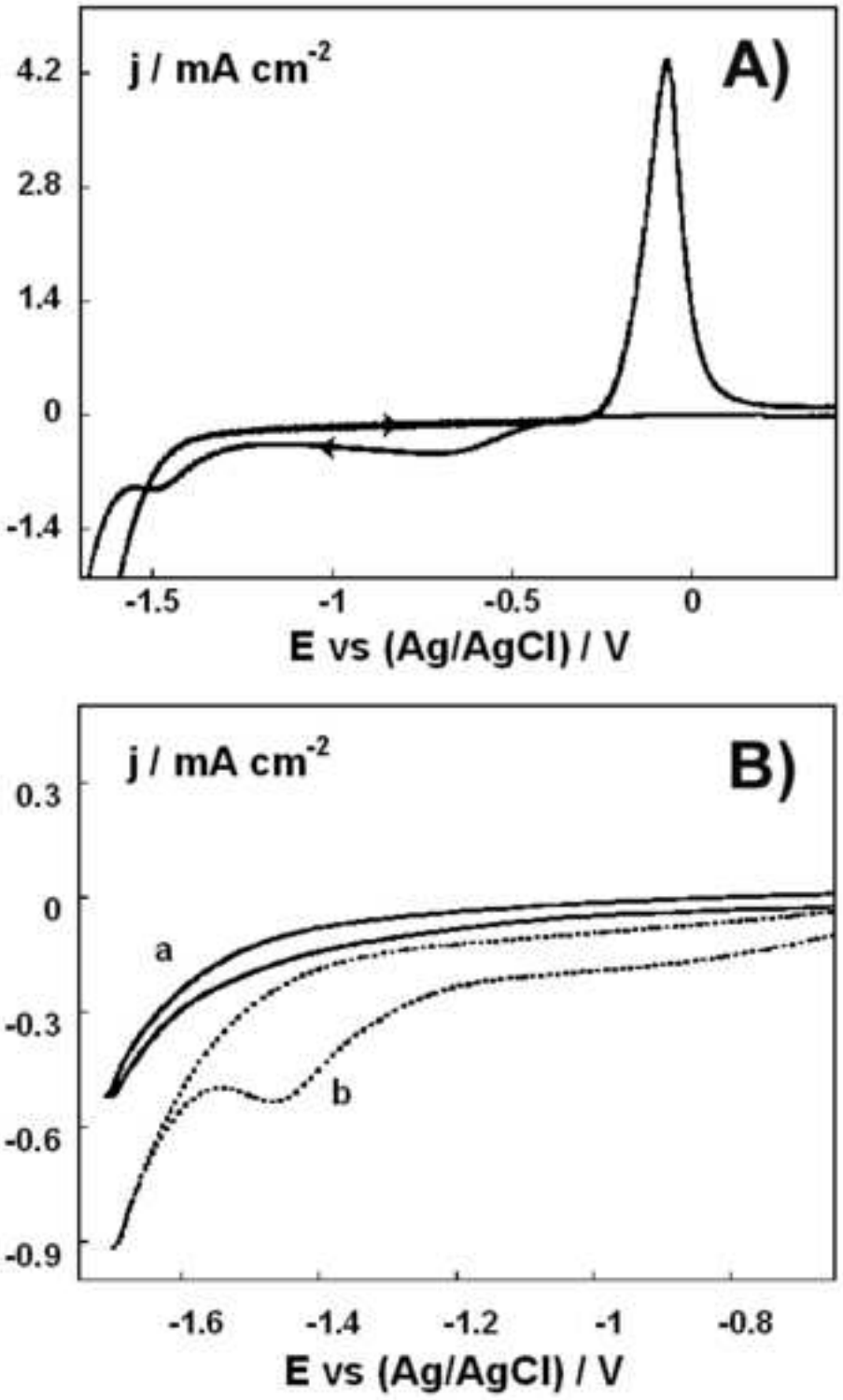

Figure 8

Figure 9

Click here to download high resolution image

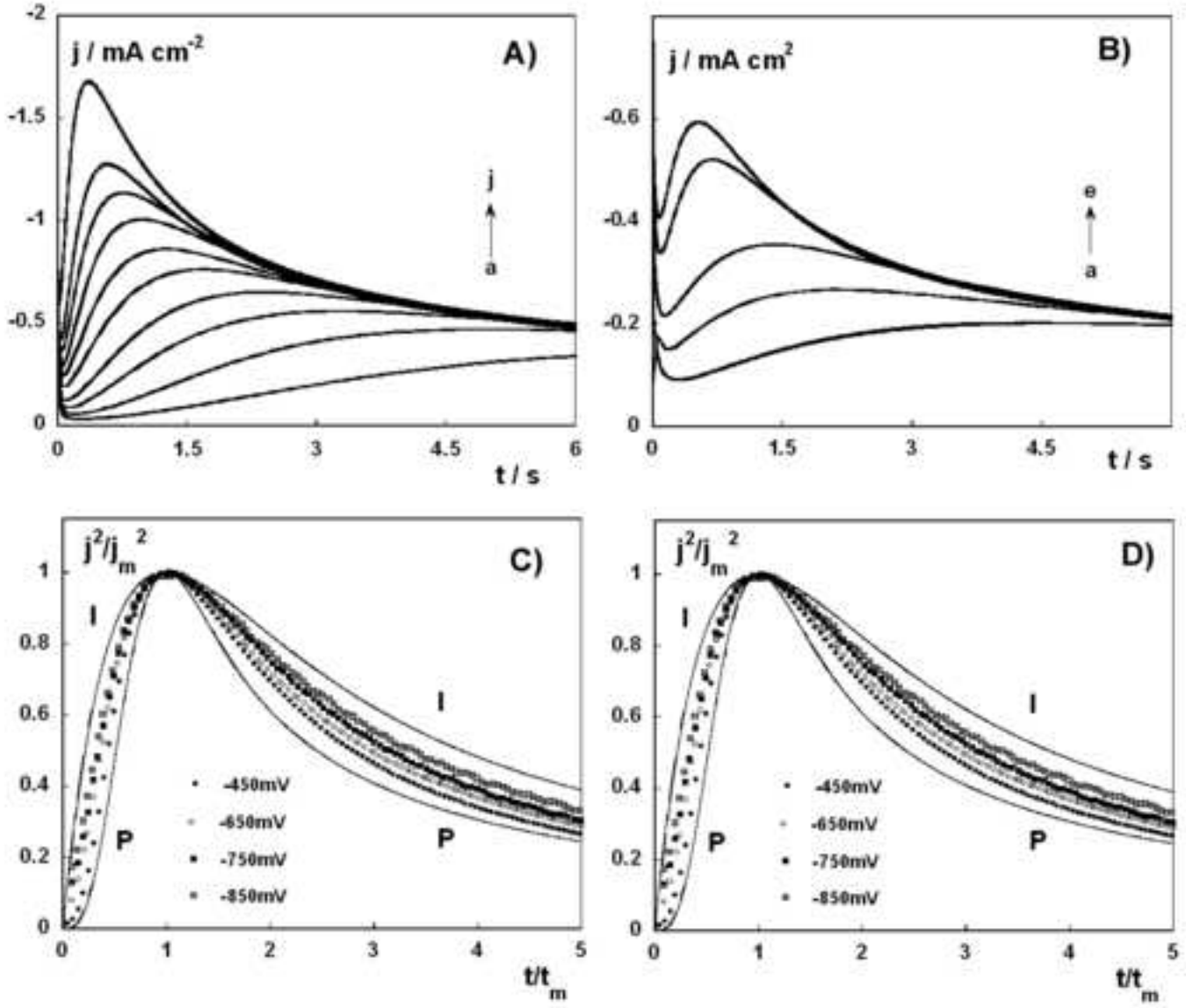

Figure 9

Figure 10
Click here to download high resolution image

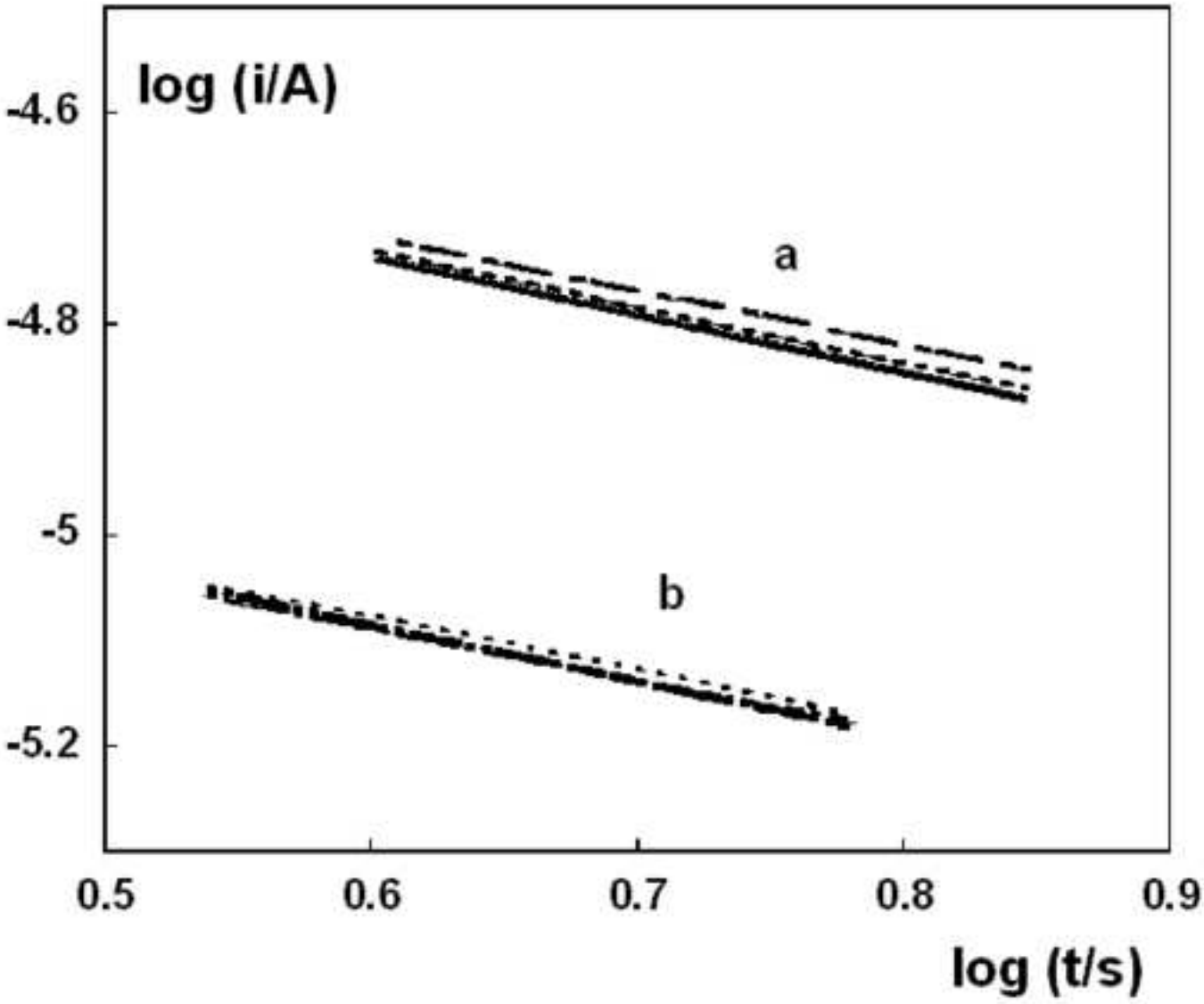

Figure 10

Figure 11
Click here to download high resolution image

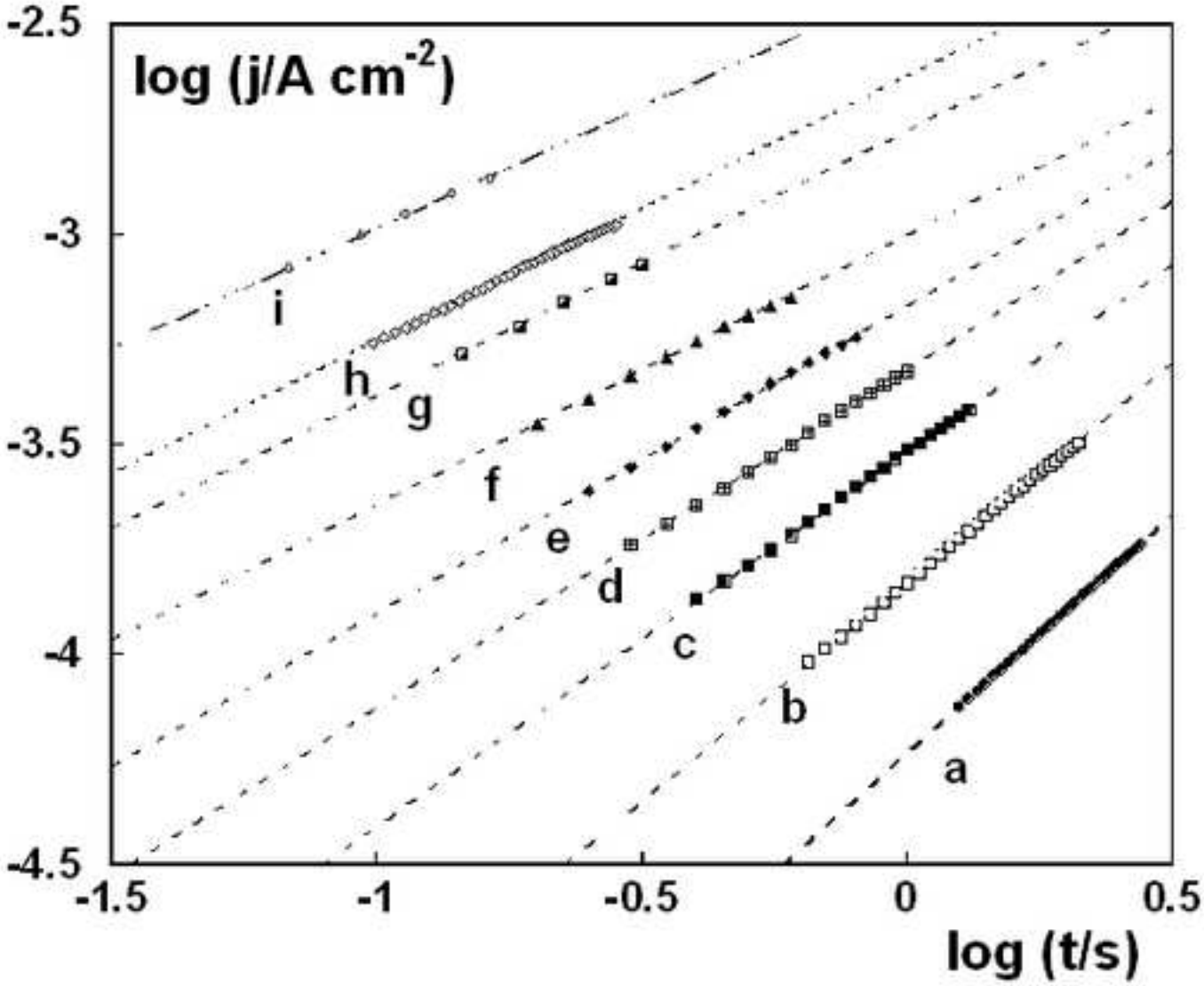

Figure 11

Figure 12ABC

Click here to download high resolution image

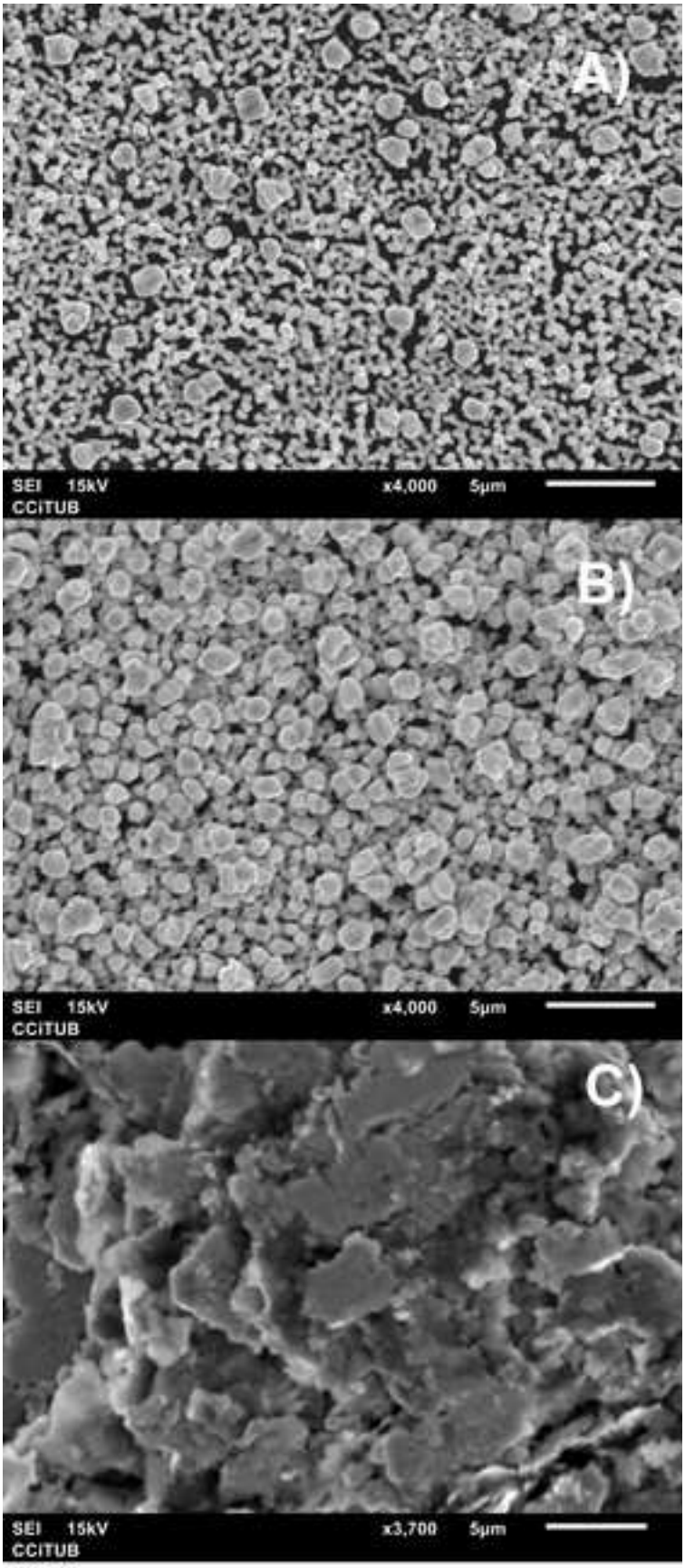

Figures 12A,B and C

Figure 12DE

Click here to download high resolution image

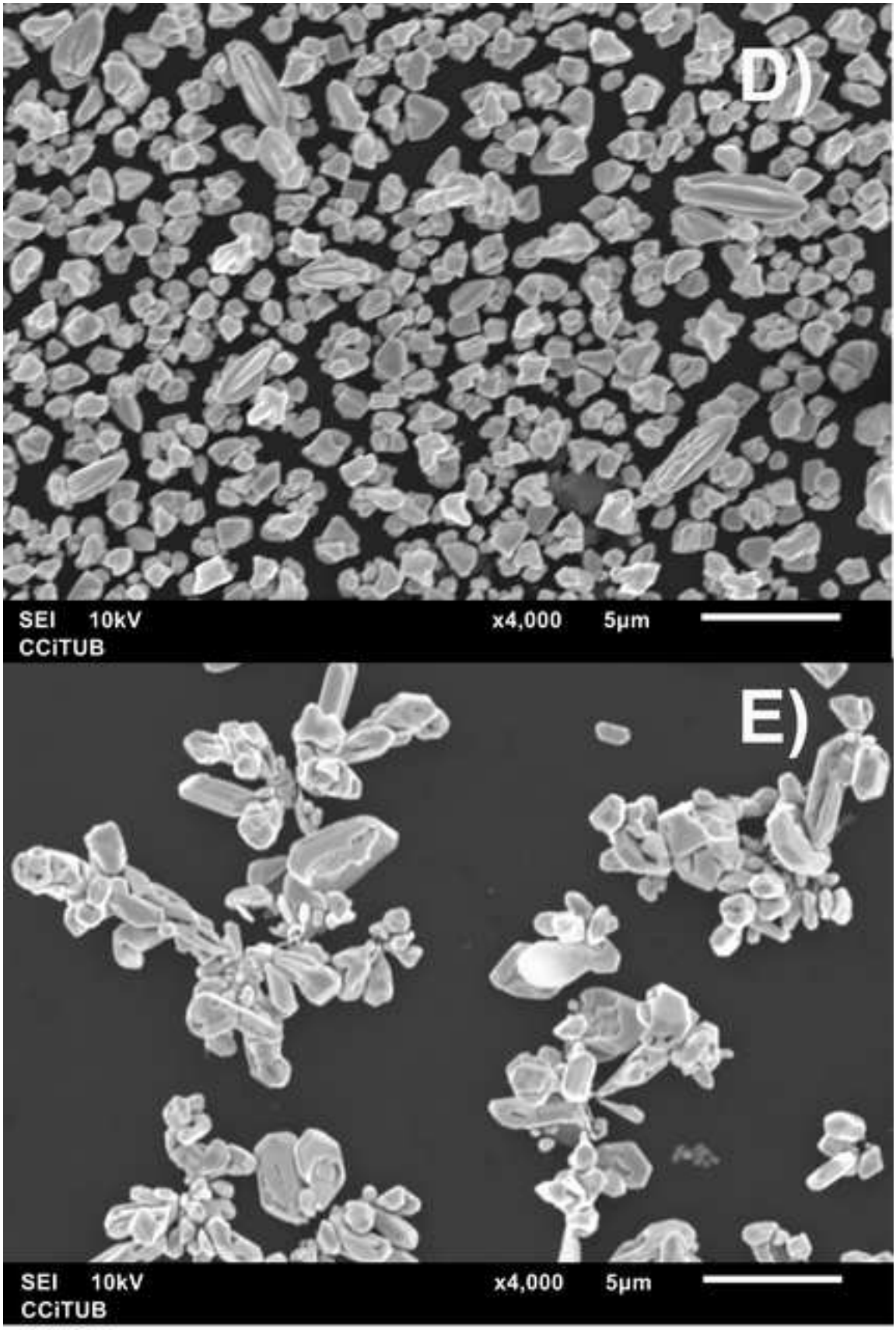

Figures 12 E and D

Figure 13
Click here to download high resolution image

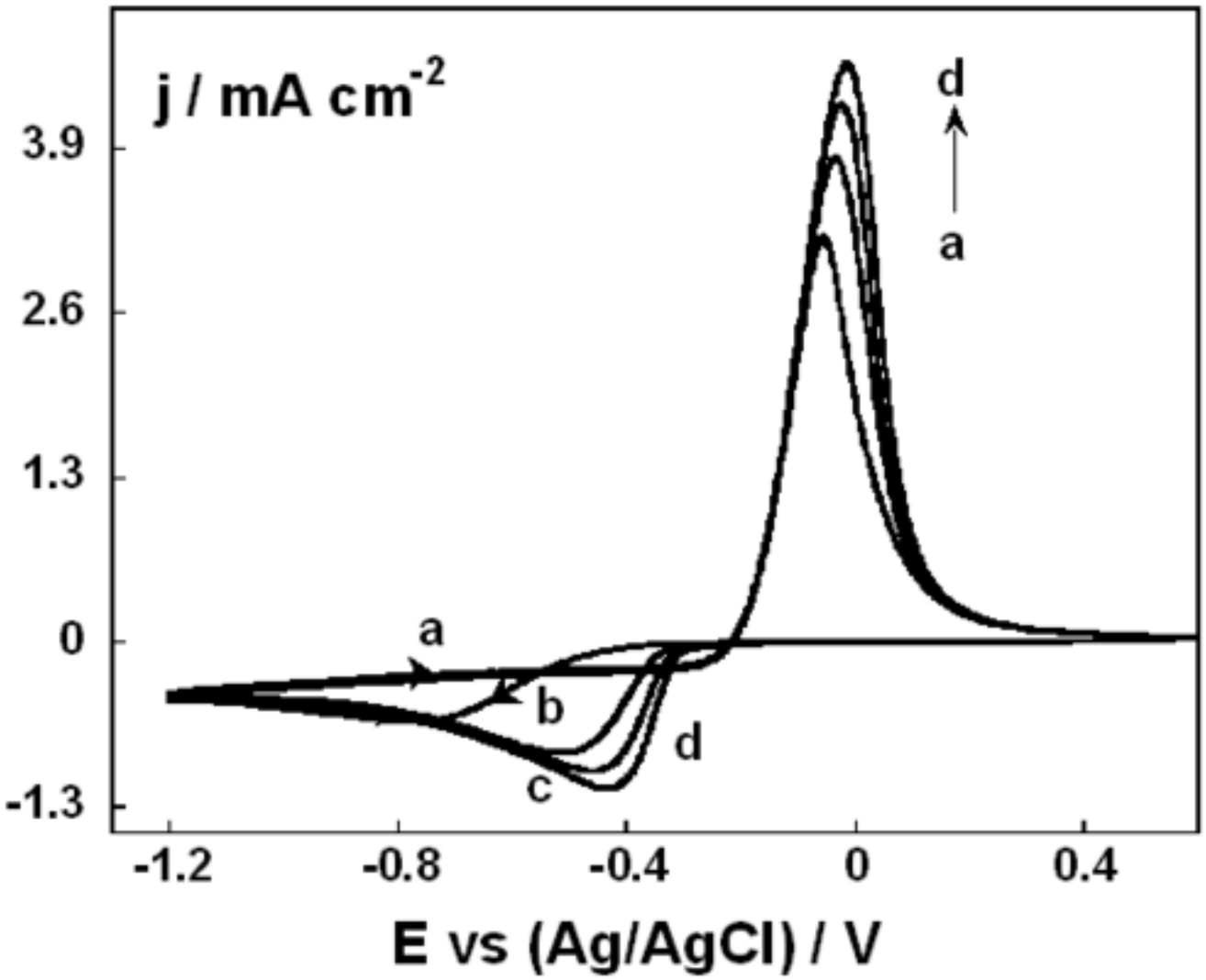

Figure 13

Figure 14
Click here to download high resolution image

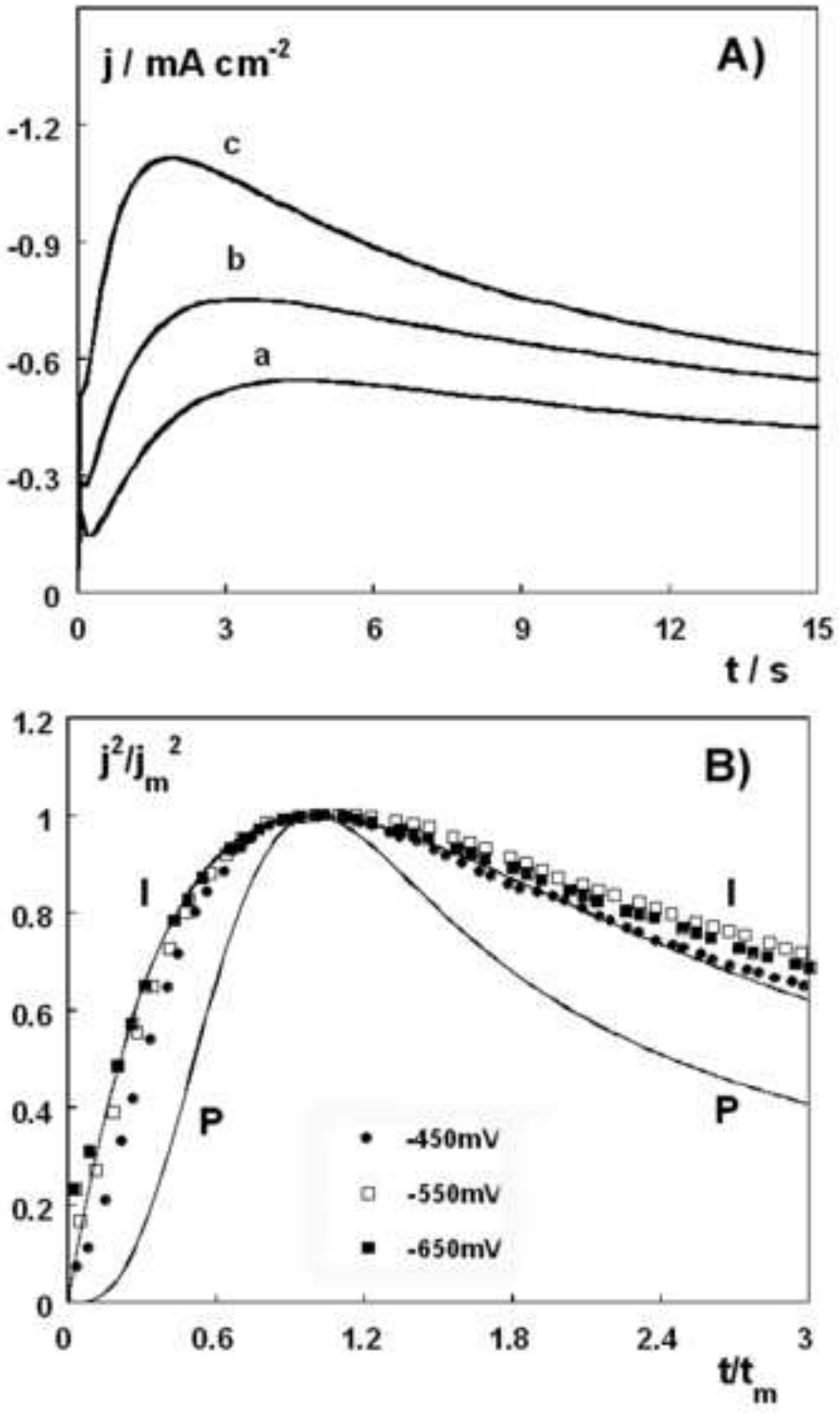

Figure 14